

Available at [www.sciencedirect.com](http://www.sciencedirect.com)journal homepage: [www.elsevier.com/locate/ije](http://www.elsevier.com/locate/ije)

# Unexpected large hydrogen adsorption by Nb cluster films under mild conditions of pressure and temperature

C.P. Romero<sup>a,\*</sup>, R.A. Trabol<sup>b</sup>, J.I. Avila<sup>b</sup>, P. Lievens<sup>a</sup>, A.L. Cabrera<sup>b</sup>

<sup>a</sup>Laboratory of Solid State Physics and Magnetism, Katholieke Universiteit Leuven, Celestijnenlaan 200D – bus 2414, B-3001 Leuven, Belgium

<sup>b</sup>Laboratorio de Ciencia de Materiales, Facultad de Física, Pontificia Universidad Católica de Chile, Santiago, Chile

## ARTICLE INFO

### Article history:

Received 10 April 2011

Received in revised form

9 July 2011

Accepted 24 July 2011

Available online 19 August 2011

### Keywords:

Niobium

Clusters

Optical properties

Hydrogen

Palladium

Electrical properties

## ABSTRACT

Hydrogen absorption in several cluster assembled films was investigated by the optical and electrical response of the films when modified by hydrogen adsorption. The films were grown by deposition of niobium clusters and by co-deposition of niobium clusters with manganese or palladium clusters on sapphire and then capped by a thin Pd film. Unusual high adsorption of hydrogen by Nb clusters and thin metal oxide reductions at room temperature can be inferred by changes in optical transmission and resistance of the film. On the other hand, no hydrogen absorption can be inferred in the same experiments with co-deposited clusters of Nb and Pd and co-deposited clusters of Nb and Mn. The technique used in this work allows fast screening and detection of potential perm-selective materials for hydrogen.

Copyright © 2011, Hydrogen Energy Publications, LLC. Published by Elsevier Ltd. All rights reserved.

## 1. Introduction

The extensive use of hydrogen gas for numerous applications is a short term goal in many governmental energy programs [1]. Some of the active areas of research in these programs are hydrogen storage and perm-selective membranes. The use of hydrogen as a fuel in automobiles is possible due to liquid hydrogen tanks, compressed hydrogen at high pressure, or the use of a fine powder called metal hydride to absorb hydrogen gas. At present, there are very few prototype vehicles running with hydrogen because hydrogen storage tanks for liquid hydrogen are very expensive and they are capable of holding hydrogen for merely two to four days. Other types of storage devices are still under development [2,3]. Palladium (Pd) is a metal that was extensively studied as the first

commercial hydrogen solid membrane in many applications [4]. Pd absorbs hydrogen without the need of high pressures (from  $10^{-4}$  to  $10^5$  Pa) and without the need of high temperatures (from 150 to 300 K) requiring a very small activation energy for the process [5]. Hydrogen is released from Pd by just removing the hydrogen atmosphere from Pd without spending energy, in other words by a pressure “swing”. For this reason, Pd-based materials have been used in hydrogen purification, tritium separation, and dehydrogenation reactions [4]. This singular metal has shed light on the development of light weight hydrogen containers using powder of metal hydride, which is hydrogen absorbed inside the solids [6]. The use of Pd for multiple applications has been limited because Pd suffers severe hydrogen embrittlement [7]. Due to this, research in hydrogen permeation has been focused on Pd

\* Corresponding author.

E-mail addresses: [christian.romero@fys.kuleuven.be](mailto:christian.romero@fys.kuleuven.be), [cpromerov@gmail.com](mailto:cpromerov@gmail.com) (C.P. Romero).

alloys and Pd-based supported membranes [8]. Numerous studies of other hydrogen–metal systems [9] have been motivated by this and other technological applications. A fundamental understanding of the easy permeation of hydrogen into Pd and the latter's high absorption capacity (two H atoms for each Pd primitive cell) is essential in order to improve hydrogen absorption properties through modification of other metals or alloys.

The high solubility of hydrogen in Pd under standard conditions of pressure and temperature results in dramatic changes in its physical and structural properties. Auer and Grabke [10] were among the first researches to study change of electrical resistance of Pd when absorbed hydrogen. We studied changes in the crystallographic orientation in the Pd grains of polycrystalline foils after undergoing several cycles of hydrogen absorption and desorption [11].

One important drawback associated with the use of Pd in any industrial application is the high cost and scarcity of this metal. It would be ideal to replace Pd by other transition metals which are more abundant and therefore less expensive. The use of other metallic films, even when coated with Pd, has not given very promising results for hydrogen storage or permeation applications. The interaction of molecular hydrogen with other metallic surfaces such as Ni, Fe, Nb, Ta, and V has also been extensively studied [12]. The absorption of hydrogen by these metals is negligible under ambient conditions. Firstly, because the dissociation of the hydrogen molecule on the surface is blocked by a native oxide, which is usually difficult to remove and secondly, in cases such as Fe and Ni the dissociation of hydrogen is endothermic and the diffusion of atomic hydrogen into the lattice is thermodynamically unfavorable. The study of hydrogen adsorption on sputter-cleaned metal surfaces performed under high vacuum conditions has been conducted over the last 40 years and the results of these studies have established that hydrogen remains chemisorbed mainly on the surface without diffusing into the bulk of many transition metals [12]. In the case of Nb, diffusivity of hydrogen in Nb is not so different than that in Pd [9], although the amount of hydrogen absorbed by Nb is controlled by the low solubility at equilibrium conditions. Pryde and Titcomb [13,14] studied the thermodynamics of hydrogen absorption by Nb filaments at low partial pressures of hydrogen ( $10^{-5}$ – $1$  Pa) and they determined an expression for the hydrogen concentration in the metal in equilibrium at a given pressure. We calculated this concentration under our experimental conditions (exposures at  $10^{-4}$  Pa and 343 K) and found that it is less than 0.8 atom%, which means that the hydrogen solubility in Nb is about 63 times less than in Pd. They also were able to obtain a desorption energy of about 58.6 kJ/mol (14 kcal/mol). Pick et al. [15,16] claimed that they were able to activate the Nb surface using a thin overlayer of Pd. According to their results they were successful in detecting large amounts of hydrogen diffusing into the Nb film at 455 K using techniques based on the change of film resistance. They determined that the desorption energy of hydrogen from pure Nb foils was 104.6 kJ/mol (25 kcal/mol), and this was decreased to 90.8 kJ/mol (21.7 kcal/mol) for Pd capped Nb foil. Strongin and his research group [17] mapped the Nb/H phases in thin 20 nm Nb films capped by 10 nm Pd film using X-ray diffraction (XRD). They claim the observation of a high density phase with 50 atom% hydrogen concentration in

Nb. Our absorption experiments using pure Nb surfaces [18] and Pd capped Nb films [19] have shown negligible hydrogen absorption in contradiction with Strongin's results.

Thin films formed by metal clusters and covered with an overlayer of palladium constitute an attractive alternative for hydrogen storage or perm-selective membranes. Cluster films have displayed new physical and chemical properties [20] not present in bulk materials, hence they have opened new interesting possibilities for applications. In particular, few atom clusters exhibit strongly size-dependent properties, with sizes corresponding to a specific number of atoms, called "magic numbers", showing strongly enhanced stability. There are many published theoretical structure calculations of metallic clusters which predict that a cluster with a small number of atoms presents structures very different from the typical crystallographic structure of the bulk metal [21–23]. Xing et al. [24] have synthesized Ag clusters containing 36–43 atoms and also Ag<sub>55</sub> (magic number) and determined their structure by trapped ion electron diffraction. They indeed found that Ag<sub>55</sub> has an icosahedral structure, while the clusters containing a smaller number of atoms have slightly distorted decahedral symmetry. Metallic clusters have relevance in areas such as developing catalytic converters and solar cells [25]. The production of metallic clusters in the gas phase has been studied for many years, and is still being studied today. Presently, many types of gas phase cluster sources are available [26] and deposited cluster properties, ranging from superconductivity and optical properties to catalysis, are being investigated.

In summary, metal clusters present different crystal structures and more surface atoms than the bulk structure. Both of these properties are attractive for optimizing gas absorption capacity normalized per metal atom. For several applications, the clusters must be deposited on the surface of a substrate thus rendering the physics of the deposition process a fundamental importance [27].

Despite the aforementioned research, it is still unclear whether significant hydrogen absorption can be induced in metallic cluster layers capped with a Pd film at relatively low hydrogen pressures and room temperature conditions, which is a requirement for energy-efficient (i.e., room temperature operation) hydrogen storage materials. The absorption of hydrogen by a sample can be inferred in most cases by two factors: (1) an increase in the transmittance of light in the visible range, and (2) an increase in the resistance of the films when hydrogen absorption (in a disordered phase) has occurred. When hydrogen absorption does not take place in the film but instead the oxide of the film is reduced, a decrease in the optical transmittance is observed. In this paper we explore this issue by using optical measurements to study hydrogen absorption in cluster films of Nb and of Nb alloys, capped with Pd.

---

## 2. Experimental

### 2.1. Sample preparation

The Nb, Pd, and Mn clusters were produced in a dual laser vaporization source [28] and deposited at low energies

(<0.2 eV/atom) on polished sapphire with (0001) orientation in an ultra high vacuum deposition chamber that has a base pressure of  $10^{-8}$  Pa. Three types of sample were produced by: (i) deposition of Nb clusters (sample C-1); (ii) co-deposition of Nb and Pd clusters (sample C-2, symbol = Nb + Pd), and (iii) co-deposition of Nb and Mn clusters (sample C-3, symbol = Nb + Mn). A detailed description of this kind of deposition can be found elsewhere [29]. When depositing the various Nb clusters the source was kept between 193 K and 213 K ( $-80^{\circ}\text{C}$  and  $-60^{\circ}\text{C}$ ). He gas was pulsed into the source at 10 Hz and a pressure of  $8 \times 10^5$  Pa (8 bar) for  $\sim 100$   $\mu\text{s}$  with a pulsed supersonic valve. When producing samples each of the ablation lasers has a different target thus enabling alloying or mixing just by changing the triggering time of the lasers so that overlap of ablated material is possible or not according to the properties of the sample that is sought. In the case of the pure Nb cluster samples we simply use one single laser or both of them but both with Nb targets.

The cluster size distribution was monitored with time-of-flight (TOF) mass spectrometry [30]. Assuming spherical shapes and the corresponding Wigner–Seitz radius for the different elements, estimated cluster sizes range from 1 nm to 2.5 nm. The different elements showed somewhat different size distributions, but in all cases clusters larger than 3 nm diameter were not fabricated. Apart from the size estimation we can also determine whether alloying is occurring when two different elements are being ablated simultaneously by careful analysis of the recorded mass spectra. In the case of sample C-2 alloying occurred. This is illustrated in Fig. 1 where TOF mass spectra are shown for the small sizes where the different cluster compositions can be disentangled. The upper trace in Fig. 1 corresponds to the Nb + Pd production. Just after the  $\text{Nb}_4$  peak there are two broader peaks, corresponding to  $\text{Nb}_3\text{Pd}$  and  $\text{Nb}_3\text{OPd}$ . These peaks are broader due to the natural isotopes of Pd. These broader peaks are absent in the case of pure Nb cluster production, as is shown in the lower trace. For sample C-3 (Nb + Mn) no alloying was observed. In this case the samples can be considered as mixtures of pure Nb and pure Mn clusters. An overview of the characteristics of the samples is given in Table 1.

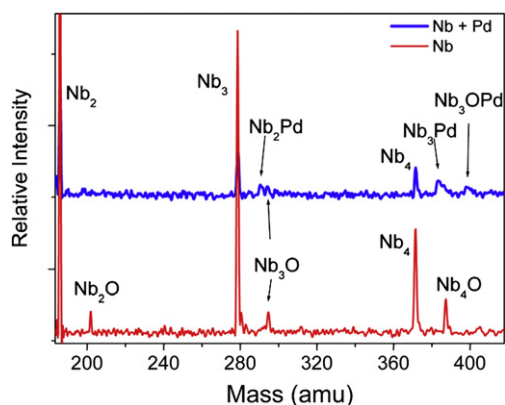


**Fig. 1** – TOF mass spectra of clusters. Upper trace is Nb + Pd. Lower trace is Nb only.

A detailed structural investigation was carried out using Atomic Force Microscopy (AFM). In Fig. 2 we show an AFM image of deposited Nb clusters without Pd capping. We estimate that the size of the nanograins resulting from the cluster deposition is 10–30 nm in lateral dimension. The height scale in the picture, ranging from dark to bright color is up to 5 nm. Thus, we estimate that the actual grain size is between 5 and 30 nm.

The Nb sputtered sample (F-1 see Table 1) was fabricated using a magnetron sputter source [19]. The target purity was >99.9%. The film was grown in an Ar atmosphere at 332 Pa. The glass substrate was cleaned using acetone, methanol, a rinse with distilled water, and dried in  $\text{N}_2$  gas.

The different materials were deposited and capped with Pd. The substrate temperature of the samples while depositing was 163 K ( $-110^{\circ}\text{C}$ ). The Pd capping layer of all samples was deposited at RT or in the process of heating up to RT, with a commercial e-beam evaporator using an ultra pure Pd rod (99.99%). Table 1 gives the Rutherford backscattering spectroscopy (RBS) thickness measurements of the samples. These thicknesses were estimated using bulk densities for Co, Mn, Nb and Pd. Our RBS resolution is  $\pm 2$  nm in estimating the layer thickness.

In order to confirm the elemental composition, the samples were characterized with RBS and XRD measurements. The RBS spectra indicate that approximately 23 atom% of the Nb cluster layer is composed of oxygen. In the case of Nb + Pd clusters it is 35 atom%. Other than variations in thickness, no other relevant differences are present in the chemical composition of the samples. The structural information as obtained from XRD shows that no relevant phase changes have occurred before or after the hydrogen exposure cycles. This means that structural changes, if any, might correspond to any amorphous phase which did not show up in the XRD pattern.

## 2.2. Optical measurements

Near-normal reflectance and transmittance measurements in the wavelength range of 400–900 nm were performed in a small cylindrical aluminum vacuum chamber equipped with two transparent quartz windows, a gas/vacuum line, and electrical feed-throughs. The incidence angle of the light is  $7^{\circ}$ . A tungsten halogen lamp was used as a source and this white light was focused on a TRIAX 180 (Jobin Yvon-Horiba) monochromator fitted with a 1200 grooves/mm diffraction grating. The light detection was done with silicon photodiodes in combination with lock-in amplifiers. The system is described in more detailed elsewhere [31]. The transmittance and reflectance experience the same relative change in the whole wavelength range measured before and after the films were exposed to hydrogen. Therefore we here present only data taken at 600 nm wavelength.

The resistance was measured with a Keithley DC resistivity bridge model 580 which allows measurements with 4 points connections. A similar system is described elsewhere [19,30]. All samples were provided with silver electrical contacts to measure the resistance simultaneously with the light transmission and reflectance. The chamber was evacuated down to 1.3 Pa using a 50 l/s Balzers turbomolecular pump. Next the chamber was filled with hydrogen reaching a pressures

**Table 1 – Samples description, thickness by RBS and transmittance values.**

| Sample | Description     | TOF alloying or mixing | RBS cluster thickness (nm) | Pd capping thickness (nm) | Transmittance film in vacuum | Transmittance film in H <sub>2</sub> | Observed $\Delta T/T$ (%) (according to Eq. (3)) | Predicted transmittance in film if only Pd capping absorbed H <sub>2</sub> (using Eq. (1) and (2)) | Predicted $\Delta T/T$ (%) if only Pd capping absorbed H <sub>2</sub> |
|--------|-----------------|------------------------|----------------------------|---------------------------|------------------------------|--------------------------------------|--|--|---|
| F-1    | Nb sputter film |                        | 14 <sup>a</sup>            | 6.5                       | 0.085 ± 0.001                | 0.090 ± 0.001                        | 6.0 ± 1  | 0.090 ± 0.001  | 6.0 ± 1   |
| C-1    | Nb cluster film |                        | 51 <sup>a</sup>            | 6.0                       | 0.032                        | 0.039                                | 24   | 0.033  | 2   |
| C-2    | Nb + Pd cluster | Alloying               | 45 <sup>a</sup>            | 27                        | 0.026                        | 0.030                                | 16   | 0.039  | 49  |
| C-3    | Nb + Mn cluster | Mixing                 | 19 <sup>a</sup>            | 15                        | 0.150                        | 0.173                                | 16   | 0.18   | 14  |

a RBS thickness estimations have a ±2 nm uncertainty.

ranging from 664 to  $1.6 \times 10^4$  Pa. As soon as hydrogen was allowed to enter the chamber, optical and electrical data were recorded during 1000 s.

### 3. Results and discussion

#### 3.1. Nb sputtered film capped with Pd

Sample F-1 (Nb sputtered film) was made as a reference in order to compare with the cluster film. Details of these experiments can be found in Ref. [19]. The transmittance of light as a function of wavelength and time was obtained for a hydrogen pressure of  $4.8 \times 10^3$  Pa. A decrease in transmittance for all wavelengths was observed. The transmittance changed from 0.094 to 0.086, or a 9% decrease, for the 600 nm wavelength in hydrogen. Our interpretation is that a Nb oxide layer is formed at the interface between Pd and Nb, which is reduced by hydrogen. This oxide reduction was also observed in an earlier study of Pd-coated Co cluster films [30]. Since water (the product of the reaction) cannot diffuse through the Pd overlayer, the most plausible explanation is that water gas is released from the edges of the sample given that there is no coating acting as a barrier at the edges.

When the hydrogen pressure was increased to  $9.8 \times 10^3$  Pa, the transmittance at 600 nm changed from 0.085 to 0.090 for a 6% increase. Since the saturation time ( $\sim 200$  s) was the same as in the case of a pure Pd film, we suspect that the transmission increase was due to hydrogen absorption by the Pd capping only. This is supported by calculating the transmittance of the bilayer as:

$$T_{\text{PdNb}} = T_{\text{Pd}} \times T_{\text{Nb}}, \quad (1)$$

which is justified because the wavelength of light used is much greater than the thickness of the films.

The transmittance of the Pd films in vacuum decreased exponentially with the thickness of the films, as expected. The transmittance of the Pd films loaded with hydrogen presented the same type of exponential decay but shifted to the right side (in the direction of increasing film thickness). Both curves can be fitted to an exponential decay of the form:

$$T_{\text{Pd}} = T_0 e^{-\beta d}, \quad (2)$$

where  $T_0$  is the transmittance for zero thickness,  $\beta$  is an absorption coefficient, and  $d$  is the film thickness. For the sample in vacuum we obtained  $T_0 = 0.70 \pm 0.02$  and  $\beta = 0.085 \pm 0.002 \text{ nm}^{-1}$ , while for the sample in hydrogen  $T_0 = 0.64 \pm 0.05$  and  $\beta = 0.067 \pm 0.004 \text{ nm}^{-1}$ . The fitting obtained was good down to 4 nm thickness with correlation coefficients of 0.999 and 0.997 for the samples measured in vacuum and hydrogen, respectively.

According to Eq. (2),  $T_{\text{Pd}} = 0.40 \pm 0.02$  for  $d = 6.5$  nm, and since  $T_{\text{PdNb}} = 0.085 \pm 0.004$ ,  $T_{\text{Nb}} = 0.22 \pm 0.02$  before hydrogen absorption. Similarly,  $T_{\text{PdH}_x} = 0.42 \pm 0.02$  for  $d = 6.5$  nm and since  $T_{\text{PdH}_x\text{Nb}} = 0.090 \pm 0.004$ ,  $T_{\text{Nb}} = 0.21 \pm 0.02$  after hydrogen absorption. Therefore, the 6% increase in the Pd/Nb bilayer is a result of hydrogen absorption in the Pd layer only.

Assuming that the Nb–H system is within the regime where Sievert's Law applies [10], the change in transmittance should have a linear relationship with the square root of the

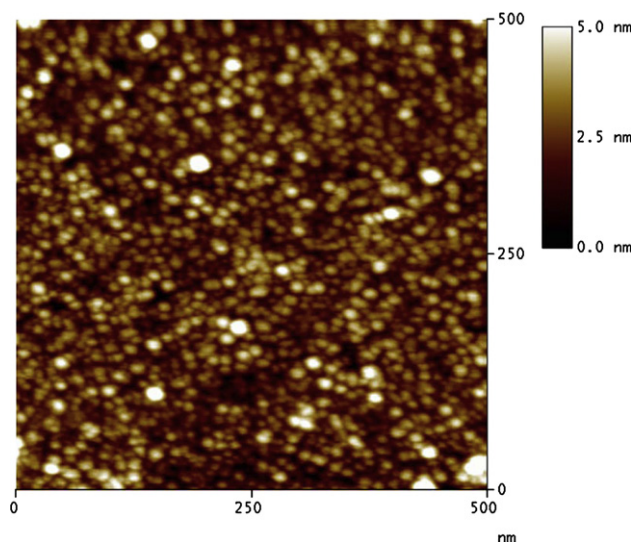


**Fig. 2 – Representative AFM image of bare Nb clusters deposited at room temperature. Image is taken without the Pd capping layer.**

hydrogen pressure. In the best case scenario, Nb would absorb 2% of atomic hydrogen. A 25% change in transmittance in the Pd layer corresponds to roughly 50% of atomic H absorption. Thus, a change in transmittance for Nb would correspond to only a 2% change in transmittance, which we were unable to detect. Our results are consistent with a hydrogen depth profile performed at room temperature in a 50 nm thick Nb film exposed to hydrogen at 500 K (226.8 °C) using the  $^1\text{H}$  ( $^{15}\text{N}$ ,  $\alpha\gamma$ ) $^{12}\text{C}$  nuclear resonance reaction, which showed that the absorbed hydrogen is concentrated at a depth smaller than 10 nm [32].

### 3.2. Nb cluster film capped with Pd

Transmittance, reflectance, and resistance measured on sample C-1 are shown in Fig. 3. The relative change in transmittance (in %) is defined as

$$\frac{\Delta T}{T} \times 100 \equiv \frac{T(P_{\text{H}}) - T(0)}{T(0)} \times 100, \quad (3)$$

where  $T(P_{\text{H}})$  is the transmittance of the Nb cluster film loaded with hydrogen and  $T(0)$  is the transmittance of the cluster film in vacuum. The relative resistance ( $\Delta R$ ) and the relative reflectance ( $\Delta\rho$ ) are defined in the same way as Eq. (3). These properties, shown in Fig. 3A, are for the first exposure of the sample to hydrogen. Fig. 3B is representative of the behavior of the sample at the second exposure to hydrogen and this behavior remains unchanged for subsequent exposures to hydrogen.

Looking at Fig. 3A, we notice that there is an unusual behavior taking place from vacuum until about  $1.6 \times 10^3$  Pa. When the Nb clusters are exposed to hydrogen the transmittance of the sample decreased and the sample's electrical resistance increased. Usually, the trend is that the electrical resistance follows the transmittance behavior. A decrease in

the transmittance represents reduction of some oxide. As mentioned before, we have observed a similar behavior in the reduction of the Co clusters [30]. After the first exposure to hydrogen, the sample has been stabilized and presents a usual behavior upon hydrogen absorption as displayed in Fig. 3B. Here, the transmittance changes up to 24%. This change can be accounted for by hydrogen absorption in the Nb cluster film as well as in the Pd capping. The transmittance values are displayed in Table 1. The last column in Table 1 is the predicted transmittance change if only the Pd capping absorbs hydrogen. The prediction is about 2%, which confirms that the Nb cluster film is absorbing a large amount of hydrogen. We are unable to estimate the amount of absorbed hydrogen on the Nb clusters, when comparing to the sputtered Nb thin film (F-1, Table 1), because that sample does not absorb hydrogen at all. Further investigation into this matter is needed to quantify the amounts of absorbed hydrogen in the cluster film.

### 3.3. Nb + Pd cluster film capped with Pd

Sample C-2 was made by co-deposition of Nb and Pd clusters. Description of this sample can be found in Table 1. Transmittance, reflectance, and resistance measured on sample C-2 after the first hydrogen exposure are shown in Fig. 4A and after the second hydrogen exposure in Fig. 4B. The transmittance initially decreased indicating some oxide reduction in Fig. 4A and then increased about 15%. This change is reproduced in the second hydrogen exposure where it also reaches about 15%. The changes predicted in case only the Pd capping absorbs hydrogen is about 49% (see Table 1), so the 16% change is well below the expected change. No absorption is detected in the Nb + Pd cluster film in this sample and the Pd capping was not absorbing efficiently.

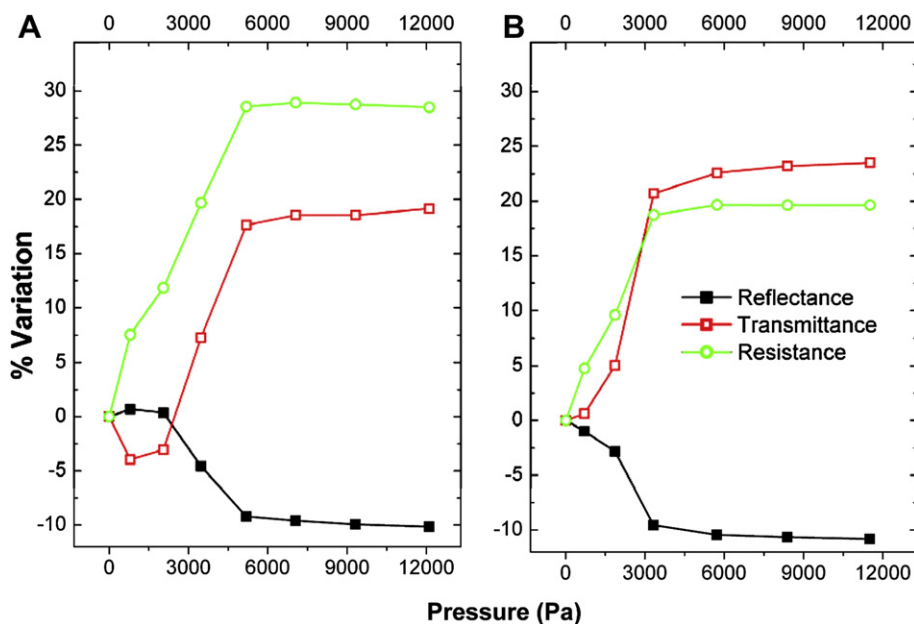


Fig. 3 – Variation of reflectance, transmittance, and resistance as a function of hydrogen pressure for Nb clusters covered with 6 nm of Pd (sample C-1). (A) First hydrogen exposure. (B) Second hydrogen exposure. Subsequent hydrogen cycles show results similar as in (B).

A second feature that is observed by this technique in the first cycle (Fig. 4A) is the transition at about  $2.1 \times 10^3$  Pa. Here, there is a rate change for the transmittance and also a “jump” in the electrical resistance. The increase in resistance might be interpreted by a decrease in electrical conduction due to a physical separation of grains in the film associated with the volume expansion of the Pd capping when it absorbs hydrogen.

Bearing in mind the combinations of phases corresponding to PdNb<sub>2</sub> and PdNb<sub>3</sub> in the TOF spectra as shown in Fig. 1, we interpret that the alloying of Pd with the Nb to form clusters inhibits the Pd from adsorbing the hydrogen. This contrasts with the results from Sample C-1 where pure Nb clusters do absorb hydrogen. Alloying Pd with Nb decreases the absorption properties of Pd and this would explain the behavior observed in sample C-2.

### 3.4. Nb + Mn cluster film capped with Pd

Sample C-3 was made by co-deposition of Nb and Mn clusters. A description of this sample can also be found in Table 1. Transmittance, reflectance and resistance measured on sample C-3 after first hydrogen exposure are shown in Fig. 5A and after the second hydrogen exposure in Fig. 5B.

No oxide reduction is observed in this sample; indeed transmittance does not decrease during the first hydrogen exposure. The behavior of sample C-3 is quite reproducible from the first to the second hydrogen exposure. The final change in transmittance is only about 16%. The predicted change assuming that only the Pd capping absorbs hydrogen is 14% (see Table 1); therefore very little hydrogen absorption happened in the Nb + Mn cluster layer. In the gas phase Nb did not alloy with Mn but alloying could occur once the different clusters are deposited and merge. We used this coagulation property to study superconductivity of Pb clusters deposited at different substrate temperatures [34].

### 3.5. Results summary

All the samples are covered with a capping layer of Palladium. According to Table 1 we can estimate the variation in the transmittance signal assuming that only this layer adsorbs hydrogen. We compare the last column labeled “Predicted  $\Delta T/T$ (%) if only Pd capping absorbed H<sub>2</sub>” in Table 1, with the column named “Observed  $\Delta T/T$  (%) (according to Eq. (3))”. Transmission change in sample F-1 coincides with the estimation of 6% change due to the Pd capping, thus revealing that the Nb layer does not adsorb any hydrogen. For sample C-1 it is estimated that we should have a change of 2% in the transmittance, while 24% is measured. This pronounced difference can be attributed to the adsorption of hydrogen by the Nb clusters. Since this behavior is due to the different production of a cluster assembled film with respect to a sputtered film, we conclude that the cluster assembled nature of the Nb is responsible for the observed huge uptake of hydrogen. Nb hydrides can be formed in Nb films [33] but large temperatures are required as well as high H<sub>2</sub> pressures. The novelty of this result is that the whole procedure is reversible: it is easy to load the Nb cluster film with H<sub>2</sub> at room temperature and as easy to desorb it. This is indeed a promising result.

Samples C-2 should have 49% of variation in the transmittance, but registered only 16%. By producing bi-metallic clusters of Nb and Pd and then depositing them and capping this film with pure Pd we expected that the adsorption of hydrogen would increase in the cluster assembled film because of the presence of Pd atoms in combination with the Nb. But the results clearly show a decrease in transmittance, possibly due to the alloying of Pd with Nb. Sample C-3 shows minimal deviation from the estimated transmittance variation due to the Pd capping. Thus the co-deposition of Mn and Nb clusters is not beneficial for hydrogen absorption.

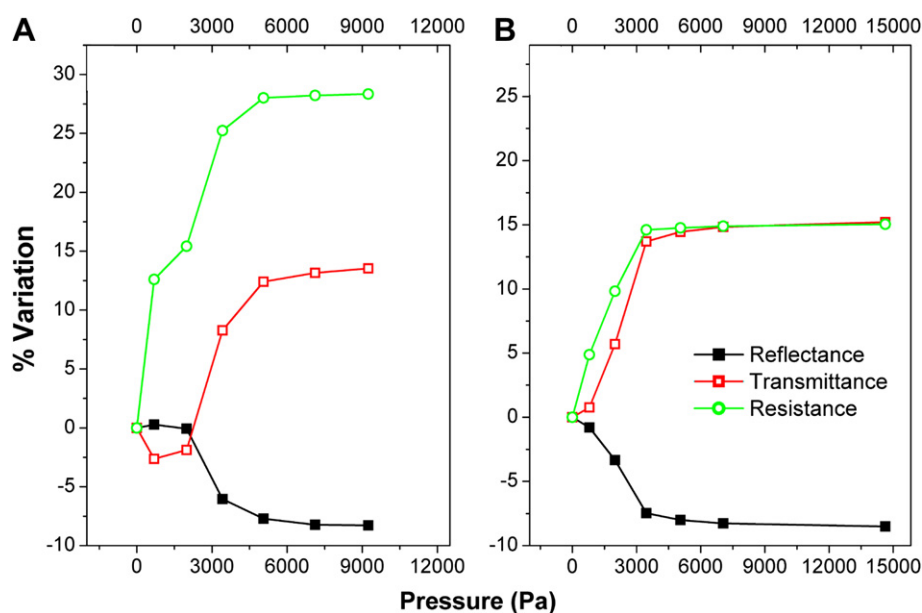
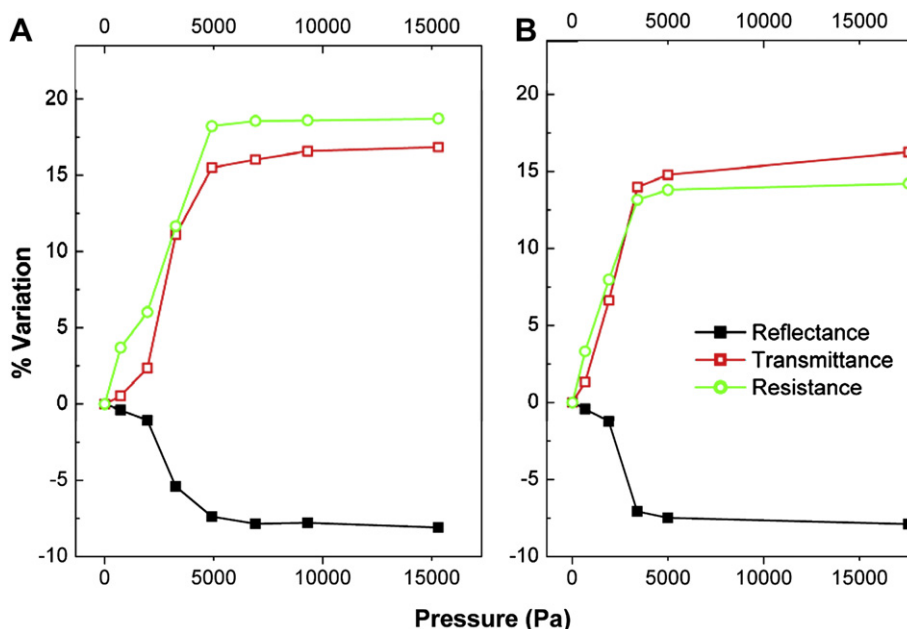


Fig. 4 – Variation of reflectance, transmittance, and resistance as a function of hydrogen pressure for Nb + Pd clusters covered with 27 nm of Pd (sample C-2). (A) First hydrogen exposure. (B) Second hydrogen exposure. Subsequent hydrogen cycles show results similar as in (B).



**Fig. 5 – Variation of reflectance, transmittance, and resistance as a function of hydrogen pressure for Nb + Mn clusters covered with 15 nm of Pd (sample C-3). (A) First hydrogen exposure. (B) Second hydrogen exposure. Subsequent hydrogen cycles show results similar as in (B).**

#### 4. Conclusions

We have studied hydrogen absorption in films using reflectance, transmittance, and changes in electrical resistance of a series of samples: films of sputtered Nb, Nb clusters, (Nb + Pd) clusters, and mixed Nb and Mn clusters, all covered with a Pd capping film. We observed that a sputtered film of Nb does not absorb hydrogen. Changing the Nb layer by a Nb cluster layer we obtain remarkable hydrogen uptake, comparable to pure Pd films, which is an unexpected result. In addition, when modifying these Nb cluster films with Pd alloying, thus forming (Nb + Pd)<sub>clusters</sub>, no absorption of hydrogen was observed. The same result was found for the case of Nb clusters mixed with Mn clusters: Mn inhibits the Nb absorbing capacity. The technique used in this work has the advantage of allowing fast scanning and detection of potential perm-selective materials for hydrogen. Effects such as oxide reduction at room temperature, which otherwise pass unnoticed when using other techniques, are detected here. Furthermore, fast and reliable comparison between samples is possible.

#### Acknowledgments

We acknowledge support by the Fund for Scientific Research-Flanders (FWO), as well as by the Flemish Concerted Action (GOA) and the Belgian Interuniversity Attraction Poles (IAP) research programs. The RBS operator Huan Wang and A. Vantomme are highly acknowledged. Grants from Departamento de Física, PUC 2010 and VRI Puente N°03/2011 are highly acknowledged.

#### REFERENCES

- [1] See for example: <http://www.hydrogen.energy.gov/>.
- [2] Dogan B. Hydrogen storage tank system and materials selection for transport applications. ASME Conference PVP2006-ICPVT-11, Vancouver, Canada, July 23–27, 2006. Conference Proceeding CD, Track: Materials and Fabrication, Session: Materials for Hydrogen Service, Paper N° 93868, pp, 1–8.
- [3] <http://www.sciencedaily.com/releases/2008>.
- [4] Armor JN. Challenges in membrane catalysis. Chemtech 1992;22:557–63.
- [5] Behm RJ, Penka V, Cattania MG, Christmann K, Ertl G. Evidence for “subsurface” hydrogen on Pd(110): an intermediate between chemisorb and dissolved species. J Chem Phys 1983;78:7486–90.
- [6] Sakintuna B, Lamari-Darkrim F, Hirscher M. Metal hydride materials for solid hydrogen storage: a review. Int J Hydrogen Energy 2007;32:1121–40.
- [7] Chen SC, CaryatHung CY, Tu CG, Rei MH. Perturbed hydrogen permeation of a hydrogen mixture-new phenomena in hydrogen permeation in Pd membranes. Int J Hydrogen Energy 2008;33:1880–9.
- [8] Tosti S. Supported and laminated Pd-based metallic membranes. Int J Hydrogen Energy 2003;28:1445–54.
- [9] Alefeld G, Volk J, editors. Topics in applied physics: hydrogen in metals I. Berlin: Springer-Verlag; 1978.
- [10] Auer W, Grabke HJ. Kinetics of hydrogen absorption in palladium (alpha-phase and beta-phase) and palladium-silver-alloys. Phys Chem Chem Phys 1974;78:58–67.
- [11] Cabrera AL, Morales-Leal E, Hasen J, Schuller IK. Structural changes induced by hydrogen absorption in palladium and palladium-ruthenium alloys. Appl Phys Lett 1995;66:1216.
- [12] Menzel D. In: Gomer R, editor. Desorption phenomena in interaction on metal surfaces. Berlin: Springer-Verlag; 1975. p. 118.

- [13] Pryde JA, Titcomb CG. Phase equilibria and kinetics of evolution of dilute-solutions of hydrogen in niobium. *J of Phys part c Solid State Phys* 1972;238:1293. doi:10.1088/0022-3719/5/12/009.
- [14] Pryde JA, Titcomb CG. Thermodynamic data of hydrogen-niobium system. *J of Phys Part C Solid State Phys* 1972;238:1301. doi:10.1088/0022-3719/5/12/010.
- [15] Pick MA, Davenport JW, Strongin M, Dienes GJ. Enhancement of hydrogen uptake rates for nb and ta by thin surface overlayers. *Phys Rev Lett* 1979;43:286–9.
- [16] Pick MA. Kinetics of hydrogen absorption-desorption by niobium. *Phys Rev B* 1981;24:4287–94.
- [17] Reisfeld G, Jisrawi NM, Ruckman MW, Strongin M. Hydrogen absorption by thin Pd/Nb films deposited on glass. *Phys Rev B* 1996;53:4974–9.
- [18] Cabrera AL, Espinosa-Ganga J, Jonsson-Akerman Johan, Schuller Ivan K. Kinetics of subsurface hydrogen adsorbed on niobium: thermal desorption studies. *J Mater Res* 2002;17:2698–704.
- [19] Cabrera AL, Avila JI, Lederman David. Hydrogen adsorption by metallic films detected by optical transmittance measurements. *Int J Hydrogen Energy* 2010;35:10613–9.
- [20] Bouwen W, Kunnen E, Temst K, Thoen P, Van Bael MJ, Vanhoutte F, et al. Characterization of granular Ag films grown by low-energy cluster beam deposition. *Thin Solid Films* 1999;354(1–2):87–92.
- [21] Rogan José, García Griselda, Loyola Claudia, Orellana W, Ramírez Ricardo, Kiwi Miguel. Alternative search strategy for minimal energy nanocluster structures: the case of rhodium, palladium, and silver. *J Chem Phys* 2006;125:214708.
- [22] Shafai Ghazal, Hong Sampyo, Bertino Massimo, Rahman Talat S. Effect of ligands on the geometric and electronic structure of Au<sub>13</sub> clusters. *J Phys Chem C* 2009;113:12072–8.
- [23] Salazar Villanueva M, Romero AH, Bautista Hernandez A. Ideal strength on clusters from first principles: the Ti<sub>13</sub> case. *Nanotechnology* 2009;20:465709 (7pp).
- [24] Xing Xiaopeng, Danell Ryan M, Garzón Ignacio L, Michaelian Karo, Blom Martine N, Burns Michael M, et al. Size-dependent fivefold and icosahedral symmetry in silver clusters. *Phys Rev B* 2005;72:081405(R).
- [25] Canali L. Novel scanning probes applied to the study of nanostructures. Delft University of Technology, ISBN 90-6464-78-79; 2000.
- [26] Reinhard PG, Suraud E. Introduction to cluster dynamics. Wiley-VCH Verlag GmbH, ISBN 3-527-40345-0; 2004. p. 40.
- [27] Palmer RE. Welcome to clusterworld. *New Sci* 1997;153:38–41.
- [28] Bouwen W, Thoen P, Vanhoutte F, Bouckaert S, Despa F, Weidele H, et al. *Rev Sci Instrum* 2000;71:54.
- [29] Vandamme N, Janssens E, Vanhoutte F, Lievens P, Van Haesendonck C. *J Phys Condens Matter* 2003;15:S2983.
- [30] Romero CP, Avila JI, Trabol RA, Huan Wang, Vantomme A, Van Bael MJ, et al. Pd as a promoter to reduce Co cluster films at room temperature. *Int J Hydrogen Energy* 2010;35:2262–7.
- [31] Avila JI, Matelon RJ, Trabol R, Favre M, Lederman D, Volkmann UG, et al. Optical properties of Pd thin films exposed to hydrogen studied by transmittance and reflectance spectroscopy. *J Appl Phys* 2010;107:1–5. 023504.
- [32] Johansson E, Olsson S, Chacon C, Hjørvarsson B. Solubility of hydrogen at low concentrations in thin epitaxial Nb(110) films. *J Phys Condens Matter* 2004;16:1165.
- [33] Reilly JJ, Wiswall Jr RH. The higher hydrides of vanadium and niobium. *Inorg Chem* 1970;9(7):1678.
- [34] Cuppens J, Romero CP, Lievens P, Van Bael MJ. Superconductivity in Pb cluster assembled systems with different degrees of coagulation. *Phys Rev B* 2010;81:064517.